^{1}H NMR Investigation of the Influence of Interacting Sites on the Dynamics and Thermodynamics of Substrate and Ligand Binding to Horseradish Peroxidase†

Gerd N. La Mar,*,‡ Griselda Hernández,‡ and Jeffrey S. de Ropp§

Department of Chemistry and Nuclear Magnetic Resonance Facility, University of California, Davis, California 95616

Received April 14, 1992; Revised Manuscript Received July 9, 1992

ABSTRACT: The influence of substrate benzhydroxamic acid (BHA) and iron ligand (cyanide) on the thermodynamics and dynamics of each of the two binding sites of horseradish peroxidase (HRP) isozyme C has been investigated by ^{1}H NMR spectroscopy. A combination of line-width analysis and saturation transfer spectroscopy has allowed the direct determination of the off-rate of substrate and ligand in the absence or presence of the other. These off-rates, together with available dissociation constants obtained by optical spectroscopy (Schonbaum, 1973), provide estimates for k_{on}. The dissociation constant for cyanide binding to the BHA·HRP complex was also directly determined by NMR. In all cases the ^{1}H NMR determined dynamic and thermodynamic data agree well with those values available in the literature. BHA binding leads to a 200-fold decrease in CN^- affinity that arises from a factor >10 decrease in $k_{off}(CN^-)$ and $>2 \times 10^3$ decrease in $k_{on}(CN^-)$. While a portion of the decrease in $k_{on}(CN^-)$ can be rationalized by water coordination of the iron in the BHA·HRP complex, the additional decrease in $k_{on}(CN^-)$ and that in $k_{off}(CN^-)$ indicates that BHA in the binding pocket blocks the CN^- ligation channel and serves as a "gate" to CN^- exchange. This view is supported by observing a factor >4 decrease in distal His labile proton exchange with bulk water in HRP–CN upon BHA binding. The ternary complex BHA·HRP–CN is shown to be heterogeneous. While the thermodynamics of BHA and CN^- binding appear similar in the two ternary complexes, the BHA on- and off-rates for the two complexes differ by a factor of ~10. The two heterogeneous forms interconvert at 25 °C at $\sim 2 \times 10^2$ s^{-1}, precluding the determination of any difference in the CN^- binding rates by saturation transfer. The greater lability of one of the two ternary complexes is attributed to an alternate orientation of some distal residue that blocks the substrate binding channel in one of the forms. Transferred nuclear Overhauser effects from the heme to BHA in the ternary complex reveal that the BHA substrate is in contact not only with the heme pyrrole D substituents but also with the distal His 42, indicating that the polar side chain of BHA extends well into the distal heme pocket. Hence it does not appear that heme peroxidase substrates need to be sterically blocked from the iron binding site to account for the failure to transfer the ferryl oxo group to most substrates. A model for the binding of BHA to HRP is presented where the hydroxamine acid proton hydrogen bonds to the distal His 42. This model accounts for the unique difference in binding constants to HRP and HRP–CN for BHA relative to other substrates and suggests a structural basis for the optimal role of aromatic peracids in activating HRP.

Horseradish peroxidase, HRP, a 42-kDa glycoprotein containing a single protohemin, is a typical member of the plant peroxidases that serve as bactericides (Dunford & Stillman, 1976; Dunford, 1991; Welinder, 1992). In common with many other heme peroxidases, it is oxidized by two equivalents by peroxides, and it carries out one-electron oxidation on a number of aromatic substrates. HRP can also carry out a two-electron oxidation of some inorganic ions such as I^- and SCN^- which bind to HRP only at very acidic pH (Dunford & Stillman, 1976; Sakurada et al., 1987; Modi et al., 1989). In fact, HRP consists of numerous isozymes (Aibara et al., 1981, 1982), of which the dominant basic isozyme C has been the most extensively studied. Detailed crystallography on the related bacterial cytochrome *c* peroxidase, C*c*P, has revealed a series of hypothesized catalytically key residues such as the proximal His and the distal His and Arg which can account for the reaction of the peroxide to yield the doubly oxidized compound I (Poulos & Kraut, 1980; Finzel et al., 1984). An X-ray crystal structure of HRP isozyme E5 is in progress, but the current limited resolution reveals only its polypeptide folding pattern (Morita et al., 1991). Sequence homology between C*c*P and HRP has implicated similar residues in the active site for the latter protein (Welinder, 1985; Welinder & Norskov-Lauritsen, 1986). In the absence of a high-resolution X-ray crystal structure of HRP, extensive ^{1}H NMR studies (de Ropp et al., 1984, 1991; Thanabal et al., 1987a,b, 1988a) have provided direct support for the existence of a coordinated His with extensive imidazolate character and distal His 42 and Arg 38 with dispositions relative to the heme very similar to that found in C*c*P, as illustrated in Figure 1.

Much less is known about the aromatic substrate binding pocket in HRP, and here the sequence homology with C*c*P is not useful because the latter has the protein cytochrome *c* as substrate, while the native substrates for HRP are phenols and aromatic amines. Several NMR studies have provided limits on the rates of binding of several substrates and estimates of the distance to the iron center (Burns et al., 1975; Morishima & Ogawa, 1979; Sakurada et al., 1986; Leigh et al., 1975; Schejter et al., 1976). In addition to the native substrates, HRP can bind a range of structurally related substrates or substrate analogs (Schonbaum, 1973; Schejter et al., 1976; Dunford & Stillman, 1976; Paul & Ohlsson, 1978; Dunford,

† This research was supported by a grant from the National Institutes of Health (GM 26226). The NMR Instruments were purchased in part from funds provided by the National Institutes of Health (RR-04795) and National Science Foundation (BBS-88-04739 and DIR-90-16484).

* Address correspondence to this author.

‡ Department of Chemistry.

§ Nuclear Magnetic Resonance Facility.

0006-2960/92/0431-9158$03.00/0

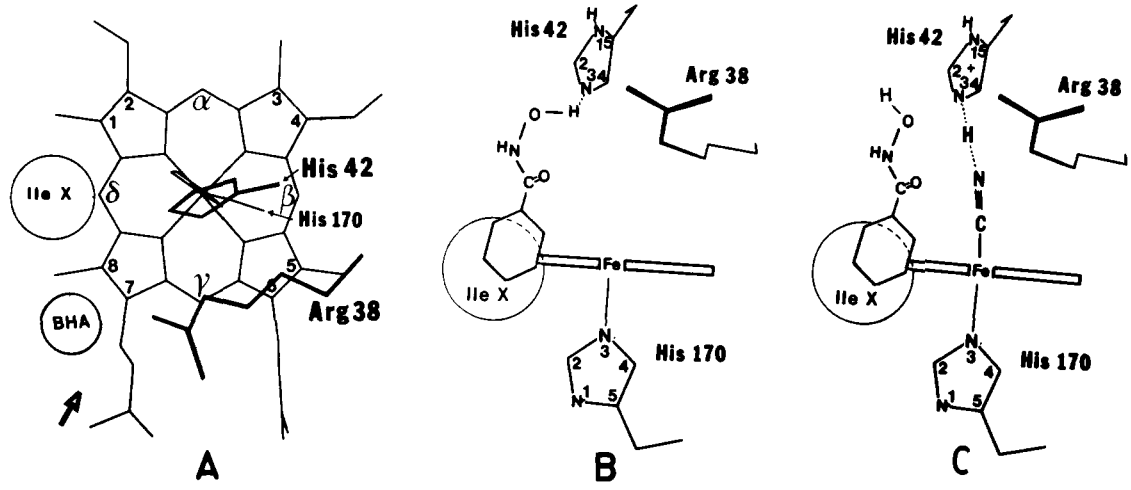

FIGURE 1: Schematic structure of the proposed active site of the BHA complex of resting-state HRP. The structure is based on the crystal structure of CcP (Poulos & Kraut, 1980) and is confirmed by ^{1}H NMR data (Thanabal et al., 1987a,b, 1988a; de Ropp et al., 1991). (A) Face-on view from the distal side and (B, C) edge-on views from the direction indicated by the arrow in (A). Included with the heme are the side chains of the axial His 170, distal Arg 38, and distal His 42. The methyl of an unidentified Ile-X is placed at the heme edge as indicated by NOEs to the 8-CH_3 and His 170 C_2H proton. The BHA substrate is placed in a position consistent with the NOE data presented in the text. The hydrogen bond from BHA to His 42 in HRP (B) is lost upon cyanide binding (C) which also protonates the imidazole side chain of His 42.

1991). The reaction with substrates involves a one-electron/one-proton transfer with either compound I or II, with the ferryl oxo group forming water. This is in contrast to heme monooxygenases (i.e., cytochrome P450), which appear to function via the same compound I intermediate but incorporate the ferryl oxo atom into the substrate (Ortiz de Montellano, 1987). This has led to the view that the substrate binding site in heme peroxidases, but not in cytochrome P450, is blocked from the reactive oxo group in the distal pocket. Elegant suicide inhibitor studies using phenylhydrazine have revealed that the phenyl group is incorporated into the chromophore solely at the δ-meso position (Ator & Ortiz de Montellano, 1987), supporting a binding pocket at (and direct electron transfer via) the heme periphery between pyrroles A and D (Figure 1). Transferred nuclear Overhauser effects, NOEs, to the substrate have been observed from the heme 8-CH_3 group in both resting state (Sakurada et al., 1986) and cyanide-inhibited HRP (Thanabal et al., 1987b; Veitch & Williams, 1991), again consistent with this heme edge binding picture.

Benzhydroxamic acid, BHA (**1**), is a structural homologue to the optimal oxidants of HRP, aromatic peracids (**2**) (Schonbaum & Lo, 1972) as well as a competing substrate of the natural phenol and aromatic amine substrates (Schonbaum, 1973). Moreover, it has been clearly established that none of the substrates bind at the heme iron (Burns et al., 1975; Sakurada et al., 1986; Schejter et al., 1976; Dunford, 1991). Hence, an elucidation of BHA binding to HRP could shed light on both activation and subsequent substrate reactions of HRP. The binding of the cyanide ligand (L) and BHA substrate (S) to the enzyme HRP (E) is described by the following equilibria with dissociation constants K_1–K_4:

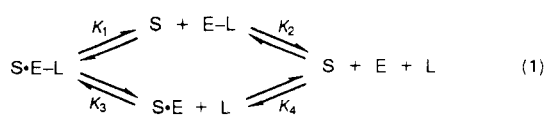

(1)

The low pH (pK ~ 4) anion binding site, which is distinct from both the cyanide binding site on the iron and the aromatic substrate binding site, is not considered here. Previous optical studies of BHA binding in the substrate pocket and cyanide binding to the heme iron had revealed that the two agents do not bind competitively, but their binding strongly interacts. Thus, three dissociations have been directly described at 25 °C: $K_1 = 1.5 \times 10^{-4}$ M (Schonbaum, 1973), $K_2 = 2.0 \times 10^{-6}$ M (Ellis & Dunford, 1968), and $K_4 = 2.4 \times 10^{-6}$ M (Schonbaum, 1973). A similar value of K_1 (6×10^{-4} M at 21 °C) has been estimated from ^{1}H NMR titration of HRP–CN with BHA (Morishima & Ogawa, 1979). Thus, it is established that BHA binding to HRP is significantly reduced upon binding cyanide.

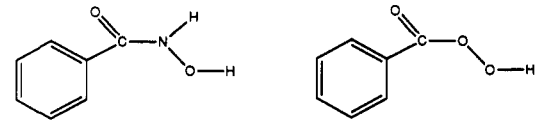

1 2

Much less information is known about the dynamic processes, k_{off}, k_{on}, which describe each of the four equilibria in eq 1. Stopped flow measurements of the second-order binding rate constant $k_{on}(CN^-) \sim 1 \times 10^5$ M^{-1} s^{-1} at 25 °C (Ellis & Dunford, 1968; Schonbaum, 1973) for K_2, and k_{on}(BHA) ~ 4×10^7 M^{-1} s^{-1} at 25 °C for K_4 (Schonbaum, 1973), have been reported, and the $k_{off}(CN^-) \sim 2.5$ s^{-1} at 55 °C for K_2 has been determined by saturation-transfer NMR (Thanabal et al., 1987a). The direct elucidation of K_3, as well as the remaining dynamic properties of the active site, is critical for a more complete understanding of the action of HRP, in particular, and heme peroxidases in general.

In addition to the rates that describe substrate and ligand binding, the dynamics of the heme pocket can be characterized by the exchange of its labile protons with bulk solvent (Woodward et al., 1982; Lecomte & La Mar, 1985). The labile proton of the distal His 42 imidazolium side chain that forms a hydrogen bond to the coordinated cyanide has been characterized in detail by ^{1}H NMR spectroscopy (Thanabal et al., 1988a). Hence, substrate binding can be expected to influence both cyanide ligation and His 42 labile proton exchange rates. For such a labile proton buried in the heme pocket, exchange with solvent is allowed only upon transient access to the pocket via local unfolding or opening of the ligation channel. Under the circumstances where the rate of the ligation channel dynamics is rapid compared to the intrinsic exchange rate of the exposed functional group, k_{ex} (the EX_2

mechanism), the relevant equation for the observed exchange rate, k_{obs}, is (Woodward et al., 1982)

$$k_{obs} = K_{op}k_{ex} \quad (2)$$

where K_{op} is the equilibrium constant for the "open" channel. For the protonated distal His 42, the intrinsic exchange rate is expected to be base catalyzed (Lecomte & La Mar, 1985), i.e.

$$k_{ex} = k_2[OH^-] \quad (3)$$

with k_2 diffusion controlled.

Information on the rates of ligand, substrate, and labile proton exchange is readily extracted from ^1H NMR spectra in the form of exchange contributions to the line width or via saturation-transfer, as described by well-known equations (Sandström, 1982). The understanding of the interplay of the dynamics of ligand, substrate, and proton exchange can be expected to provide insight into the stereochemical relationship of the various binding sites. Moreover, the necessarily paramagnetic states of both resting state ($S = 5/2$) and cyanide-inhibited ($S = 1/2$) heme peroxidase impart large hyperfine shifts to active site residues which considerably improve the spectral and temporal resolution of structural differences not readily detectable by other spectroscopies. Under favorable circumstances where resonance assignments are available, the structural changes can be localized in the heme cavity. Previous 1D and 2D NMR studies of HRP–CN have provided the assignments of both the heme and important catalytic residues (de Ropp et al., 1984; Thanabal et al., 1987a,b, 1988a; de Ropp et al., 1991).

We demonstrate herein that measurement of the thermodynamics and dynamics of BHA and cyanide binding reveal a substrate binding site that blocks the ligation channel to the iron, and hence implies the BHA binding site is, at least partially, in the distal heme pocket. This hypothesis is confirmed by transferred NOE studies of BHA binding to HRP–CN which reveal at least two binding modes which exhibit dipolar contact between BHA and the distal His 42.

MATERIALS AND METHODS

Materials. Horseradish peroxidase was purchased from Boehringer-Mannheim as a lyophilized salt-free powder and used directly without further purification; the protein is 98% isozyme C and the R_z value is 3.4. Protein samples were prepared 3 mM in 99.9% ^2H_2O. Solutions of potassium cyanide (Mallinckrodt) or BHA (Aldrich), prepared in the same solvent, were added as necessary to the protein solution to produce the desired stoichiometry of protein, ligand, and substrate. Solution pH, uncorrected for isotope effect, was adjusted with dilute ^2HCl or NaO^2H. To observe exchangeable protons, the protein solution was dissolved in 90% H_2O/10% ^2H_2O with the small amount of ^2H_2O serving for the internal lock.

NMR Measurements. Spectra of (high-spin) resting state HRP and its BHA complex were obtained at 300 MHz on a General Electric-NMR Ω-300. Spectra of (low-spin) HRP–CN and its complexes with BHA were obtained at 500 MHz on a General Electric-NMR Ω-500. The lower field strength was used for the high-spin samples due to their Curie spin relaxation (Gueron, 1975) which results in a B_0^2 dependence for the paramagnetic line width. Typical resting state HRP spectra were collected with 2048 complex points over a 60 kHz spectral width with a pulse repetition rate of 10–20 s^{-1}. HRP–CN spectra were collected with 8192 complex data points over a 40-kHz spectral width with a pulse repetition rate of 2 s^{-1}. The residual solvent line was suppressed with a low power presaturation pulse. One-dimensional, 1D, nuclear Overhauser effect, NOE, and saturation-transfer measurements were both conducted using a low-power 30-ms decoupler pulse to saturate the resonance of interest; data acquired with the decoupler on-resonance were interleaved with those acquired with the decoupler off-resonance. Selective T_1s were measured by the saturation recovery method using a decoupler pulse to saturate the resonance of interest. The recovery was determined from the initial slope of the semilogarithmic plot of $I - I_0$ vs delay time (Granot, 1982). All data were treated with exponential apodization to increase signal-to-noise; generally 5–20 Hz were employed for low-spin spectra and 20–50 Hz were employed for high-spin spectra. Peak shifts are referenced to the residual water line, which in turn had been calibrated to internal 2,2-dimethyl-2-silapentane-5-sulfonate, DSS. Overlapping resonances were deconvoluted to obtain areas and line widths using the deconvolution tool in the GE-NMR Ω-6.0 software.

Magnitude COSY spectrum of 3 mM HRP–CN in ^2H_2O with a 10-fold excess of BHA, at pH 6.8 and 40 °C, was obtained on a General Electric-NMR Ω-500 spectrometer. In order to characterize the relatively narrow resonances of the free BHA, data were collected using 512 blocks in t_1 and 1024 complex points in t_2 over a band width of 6.7 kHz with a repetition rate of 0.45 scan per second. The data set was processed on a Sun 3/260 workstation using an unshifted sine-bell-squared window function over the collected data in both dimensions, and zero-filling to 1024 × 1024 points prior to Fourier transformation.

Analysis of Dynamics. The rates of exchange processes are determined either by effects on line widths or by the transfer of saturation (Sandström, 1982). We consider exchange between resonances a and b with lifetimes τ_a and τ_b. The observed line width for peak a in slow exchange is given by

$$\delta_{obs} = \delta_a^\circ + \frac{1}{\pi\tau_a} \quad (4)$$

and for the averaged resonance in the limit of rapid exchange is

$$\delta_{obs} = f_a\delta_a^\circ + f_b\delta_b^\circ + 4\pi f_a^2 f_b^2(\Delta\nu_{ab})^2(\tau_a + \tau_b) \quad (5)$$

where f_a and f_b are the mole fraction of species a and b, δ_a° and δ_b° are the line widths of peaks a and b in the absence of exchange, and $\Delta\nu_{ab}$ is the chemical shift difference between the a and b peaks, in hertz. In the particularly convenient case where the two sites are equally populated, the mean lifetime, τ, is obtained from

$$\delta_{obs} = \frac{1}{2}(\delta_a^\circ + \delta_b^\circ) + \frac{\pi}{2}(\Delta\nu)^2\tau \quad (6)$$

Upon steady-state saturation of resonance b, the intensity of resonance a, $I_a(\infty)$, is related to its intensity in the absence of saturating $I_a(0)$, via the saturation factor, F_a, defined by

$$F_a = \frac{I_a(\infty)}{I_a(0)} = \frac{\tau_a}{\tau_a + T_{1a}} \quad (7)$$

where T_{1a} is the selective relaxation time of the a resonance in the absence of exchange.

RESULTS

Effect of BHA on CN^- Affinity. The ^1H NMR spectrum of a 3.0 mM solution of HRP 30 mM in total cyanide in ^2H_2O at 25 °C and pH 6.8 exhibits solely the peaks for the low-spin HRP–CN complex (<0.1% HRP), which is expected on the basis of the very tight CN^- binding ($K_2 = 2.0 \times 10^{-6}$ M) (Ellis

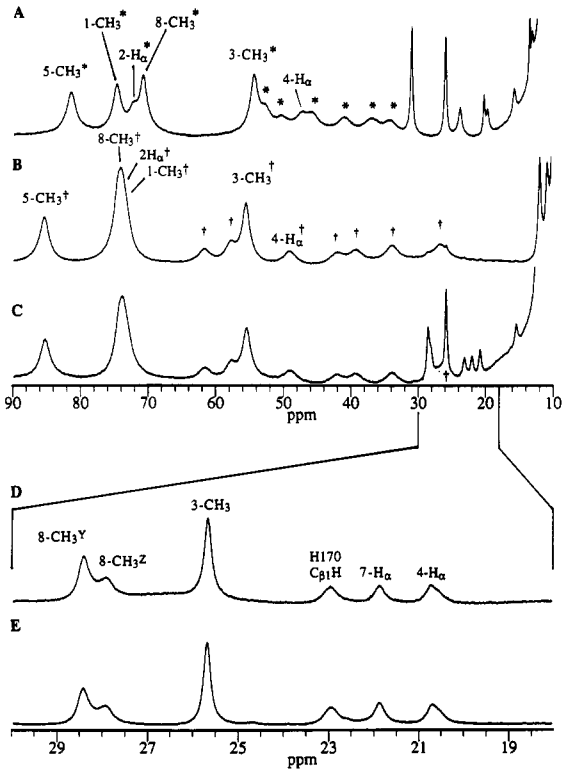

FIGURE 2: Cyanide binding to the BHA·HRP complex. The low-field resolved portions of the 300-MHz ^1H NMR trace of 3 mM HRP in ^2H_2O at 25 °C, pH 6.8 (A), containing 0.35 equivalent of CN^- to yield a ~2:1 ratio of HRP:HRP–CN; the resting-state HRP peaks are labeled by * and assignments are as reported previously (Thanabal et al., 1987a,b). (C) Sample in (A) upon the addition of a 10-fold of excess BHA. The trace for the pure BHA·HRP complex is illustrated in (B); note that a BHA·HRP resonance appears under the 3-CH_3 peak of the BHA·HRP–CN complex. Those resonances of BHA·HRP which can be brought to the fast exchange limit with HRP at 55 °C have their assignments given. The area of the 3-CH_3 peak of the BHA·HRP–CN complex relative to the 5-CH_3 peak area of the BHA·HRP in trace C is reduced by ~15% as compared to this ratio in trace A. (D) A portion of the 500-MHz ^1H NMR trace of the same sample as shown in (C), for which the improved resolution shows that the 8-CH_3 peak from the BHA·HRP–CN complex is split into two components labeled 8-CH_3^Y and 8-CH_3^Z. (E) 500-MHz ^1H NMR trace of the same sample used for trace D upon the addition of excess cyanide to yield the fully formed BHA·HRP–CN complex; note that line widths, chemical shifts, and relative areas of 8-CH_3^Y, 8-CH_3^Z peaks are unchanged from those in trace D.

& Dunford, 1968). Upon addition of a 10-fold excess of BHA to this solution (30 mM), the ^1H NMR spectrum of the low-spin complex is selectivity perturbed by BHA binding, as reported previously (Morishima & Ogawa, 1979; Thanabal et al., 1987b). Moreover, concomitant with this change is the appearance of the resonances of the high-spin BHA·HRP complex (not shown) which have also been described before (Morishima & Ogawa, 1979). The increase in population of the high-spin complex (to ~4%) dictates that CN^- binding is reduced (by ~10^2–10^3) upon BHA binding. This effect, as well as the existence of more than one form of the BHA·HRP–CN complex, is better illustrated when the cyanide is present in substoichiometric amounts. The 25 °C, pH 6.8, 300-MHz ^1H NMR spectra of 3.0 mM HRP upon addition of 0.35 equivalent of CN^-, and upon subsequent addition of excess (~10 fold) BHA to the same HRP solution with 0.35 equivalent of CN^-, are illustrated in parts A and C of Figure 2, respectively; the resting state HRP resonances are marked by an asterisk and are labeled as previously assigned (La Mar et al., 1980; Thanabal et al., 1988b; de Ropp & La Mar, 1991). The trace in Figure 2B is that of HRP in the presence of excess BHA and identifies the resonances of the BHA·HRP complex (labeled with †), as reported previously at 21 °C (Morishima & Ogawa, 1979). A 15 ± 5% decrease in the relative intensity of the 3-CH_3 peak in Figure 2C of the low-spin complex relative to the high-spin 5-CH_3 peak (see below), yields $K_3 \sim (4 \pm 1) \times 10^{-4}$ M. This directly determined value is consistent with the calculated value $K_3 = K_1K_2/K_4 = 1.2 \times 10^{-4}$ M as dictated by the interrelationship among the four equilibria in eq 1.

Inspection of Figure 2, however, reveals that the description of simultaneous CN^- and BHA binding is more complicated than that described by a single K_1. Thus the HRP–CN 8-CH_3 peak in the 300-MHz trace in Figure 2C not only is broadened also appears split into two overlapping resonances. This effect is more clearly demonstrated in the higher field 500-MHz ^1H NMR trace of the same solution in Figure 2D, where it is clear that the 8-CH_3 peak resolves into two resonances of ~3:2 intensity with the sum of the areas equal to that of the 3-CH_3 peak. *Hence there are at least two distinct BHA·HRP–CN complexes in solution.* Addition of excess CN^- to the solution which gave rise to Figure 2D yields the 500-MHz ^1H trace in Figure 2E. There are no changes in either line width or shifts upon further addition of either BHA or CN, so this spectrum describes the fully formed BHA·HRP–CN complexes. However, since neither the shifts nor line widths of the two 8-CH_3 peaks change on going from fractional to complete CN^- binding, the two environments represented by the 8-CH_3^Y and 8-CH_3^Z peaks reflect solely two forms of BHA binding to the HRP–CN complex. Moreover, since the relative intensities of the two 8-CH_3 are the same whether there is only fractional CN^- binding (Figure 2D) or complete CN^- binding (Figure 2E) to HRP with excess BHA solution, the two BHA·HRP–CN complexes have essentially the same cyanide affinity, i.e., $K_3 \sim 4 \times 10^{-4}$ M.

Effect of BHA on CN^- Dynamics. In the presence of both resting-state and cyanide-ligated enzyme, the transfer of magnetization between the two derivatives in the absence of BHA has been demonstrated to be controlled by $k_{off}(CN^-)$, as detected by saturation transfer to the low-spin heme methyl peak upon saturation of the high-spin heme methyl peak (Thanabal et al., 1987a). The ^1H NMR spectra at 55 °C, pH 6.8, of 2:1 high-spin:low-spin HRP complexes in the absence of BHA and presence of saturating BHA are illustrated in parts A and C of Figure 3, respectively. Difference spectra showing saturation of the high-spin species 3-CH_3 peak (HRP peaks are labeled by *) in the absence and presence of BHA (BHA·HRP peaks are labeled by †) are illustrated in parts B and D of Figure 3, respectively. Measurement of the selective T_1s of the low-spin complex 3-CH_3 peaks with and without BHA yields very similar values of 54 ± 5 and 43 ± 5 ms, respectively. The ~0.9 saturation factor in the absence of BHA yields $k_{off}(CN) \sim 2.6\ s^{-1}$ at 55 °C via eq 7. The significantly increased saturation factor in the presence of BHA, $F > 0.99$, demands that $k_{off}(CN^-)$ for the BHA complex is >10 times slower, or $<0.2\ s^{-1}$. Correcting for the necessarily high temperature (55 °C) of the saturation transfer measurements to 25 °C (factor 2 per 10 °C, which is based on an activation energy of 12 kcal/mol, typical for numerous ligand replacement reactions (Atwood, 1985)) yields an estimated $k_{off}(CN^-) \sim 4 \times 10^{-1}\ s^{-1}$ and $<4 \times 10^{-2}\ s^{-1}$ in the absence and presence of BHA, respectively. For pure HRP, the $k_{off}(CN^-)$, together with $K_2 = 2.0 \times 10^{-6}$ M (Ellis & Dunford, 1968), yields $k_{on} \sim 2.0 \times 10^5\ M^{-1}\ s^{-1}$ as listed in Table I. This value compares well with the optically measured value of $1 \times 10^5\ M^{-1}\ s^{-1}$ (Ellis & Dunford, 1968; Schonbaum, 1973). However, the reduced cyanide binding, $K_3 \sim 4 \times 10^{-4}$ M, together with the much slower $k_{off}(CN^-)$

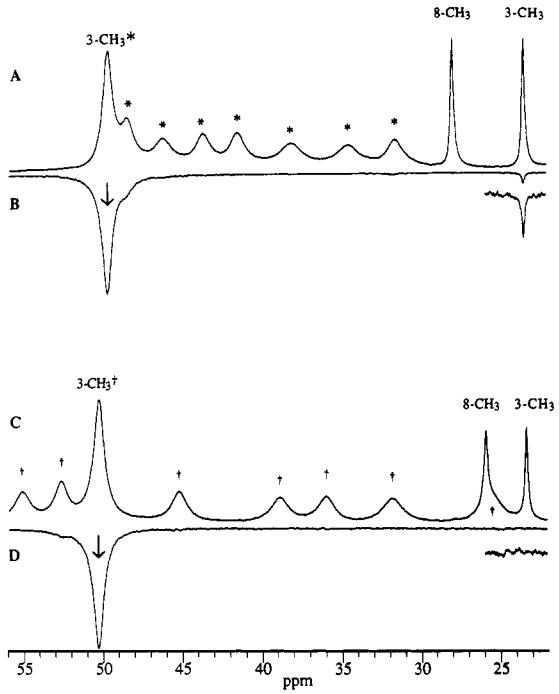

FIGURE 3: Cyanide exchange determined by ^1H saturation transfer NMR. Portion of the resolved 300-MHz ^1H NMR spectrum in ^2H_2O, pH 6.8, at 55 °C of 2:1 HRP:HRP–CN which displays the 3-CH_3 peak for both the high-spin and low-spin complexes: (A) In the absence of BHA and (C) in the presence of a 10-fold molar excess of BHA. The resonances for HRP and the BHA·HRP complex are labeled by * and †, respectively. (B) Difference trace of 2:1 HRP:HRP–CN sample in the absence of BHA, upon saturating the HRP 3-CH_3* peak. Note a ~10% saturation of the HRP–CN 3-CH_3 peak (i.e., saturation factor $F = 0.9$). (D) Difference trace of the 2:1 BHA·HRP:BHA·HRP–CN complex in the presence of excess BHA upon saturating the BHA·HRP 3-CH_3† peak; note the absence of detectable (<1%) saturation ($F \geq 0.99$) of the BHA·HRP–CN 3-CH_3 peak.

Table I: Thermodynamic and Dynamic Parameters for Ligand and Substrate Binding to Horseradish Peroxidase[a]

equilibrium	K_i[b] (M)	k_{off}[c] (s^{-1})	k_{on}[d] (M^{-1} s^{-1})
HRP–CN ⇄ HRP + CN^-	2.0×10^{-6} (K_2)[e]	4×10^{-1}	2×10^5[f]
BHA·HRP–CN ⇄ BHA·HRP + CN^-	~4×10^{-4} (K_3)[g]	$<4 \times 10^{-2}$	$<1 \times 10^2$
BHA·HRP ⇄ BHA + HRP	2.4×10^{-6} (K_4)[h]	4.0×10^2	1.7×10^8[i]
$(BHA·HRP–CN)^Y$ ⇄ BHA + HRP–CN	1.5×10^{-4} (K_1^Y)[h]	6.7×10^3	4.5×10^7
$(BHA·HRP–CN)^Z$ ⇄ BHA + HRP–CN	1.5×10^{-4} (K_1^Z)[h]	7.8×10^2	5.2×10^6

[a] At 25 °C, pH 6.8. [b] Expressed as dissociation constants; the subscript i to K_i is cross-referenced to the equilibria in eq 1 in the text. [c] Determined herein from analysis of NMR data. [d] Calculated from $K = k_{off}/k_{on}$ using data in the previous two columns. [e] From Ellis and Dunford (1968). [f] Result obtained here compares well with reported values of 1×10^5 (Chance, 1949; Ellis & Dunford, 1968) and 1.3×10^5 (Schonbaum, 1973). [g] Value determined directly here by NMR compares reasonably well to that predicted by $K_3 = K_2K_1/K_4 \sim 1.2 \times 10^{-4}$ using the values obtained by Schonbaum (1973). [h] Taken from Schonbaum (1973). [i] This value compares reasonably well to estimates of 4×10^7 M^{-1} s^{-1} reported in Schonbaum (1973).

$< 4 \times 10^{-2}$ s^{-1} at 25 °C, leads to $k_{on}(CN^-) < 1 \times 10^2$ M^{-1} s^{-1} for the BHA complex as listed in Table I. Thus, BHA binding lowers the cyanide binding constant by $\sim 2 \times 10^2$ by reducing the off-rate by a factor of >10 and the on-rate by a factor $> 2 \times 10^3$.

Effect of BHA on Labile Proton Exchange in HRP–CN. The NMR spectrum of HRP–CN at 35 °C exhibits two resolved hyperfine-shifted labile protons at 30.5 and 16.2 ppm

Table II: Chemical Shifts of Resolved Signals in HRP–CN and BHA·HRP–CN[a]

signal	HRP–CN	BHA·HRP–CN[b]		difference[c]	
8-CH_3	30.9	28.4(Y)	28.0(Z)	2.5(Y)	2.9(Z)
3-CH_3	25.9	25.7		0.2	
4-H_α	20.1	20.7(Y)	20.5(Z)	–0.6(Y)	–0.4(Z)
His 170 $C_{\beta 1}H$	23.6	22.9		0.7	
His 170 $C_{\beta 2}H$	15.5	15.3		0.2	
His 170 C_2H	–29.8	–24.7(Y)	–23.4(Z)	–5.1(Y)	–6.4(Z)
His 170 C_4H	~22.5	~18		~4.5	
His 42 C_2H	13.3	12.3		1.0	
His 42 N_3H	31.5	30.5		1.0	
His 42 N_1H	16.3	16.2		0.1	
Arg 38 $C_\beta H$	–5.5	–4.6(Y)	–4.2(Z)	–0.9(Y)	–1.3(Z)
Arg 38 $C_\delta H$	–7.0	–7.0		0	
Ile-X $C_\delta H_3$(M)	–3.2	–1.7(Y)	–1.5(Z)	–1.5(Y)	–1.7(Z)

[a] Shifts in parts per million from DSS at 25 °C, pH 6.8, for 3 mM protein in ^2H_2O, except for His 42 N_1H and N_3H, which are in ^1H_2O solution. [b] For resolved signals for the Y,Z heterogeneity, individual shifts are listed; BHA is present in a 10-fold excess. [c] Difference in shift, in parts per million, for HRP–CN minus that in BHA·HRP–CN.

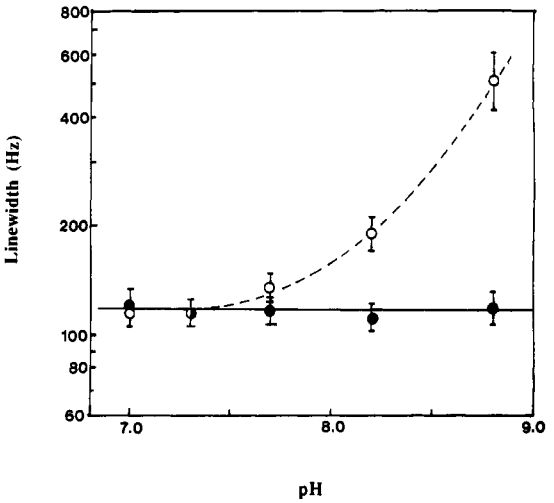

FIGURE 4: Influence of BHA binding on labile proton exchange in HRP–CN. Plot of the log of observed line width, in hertz at 360 MHz, of the distal His 42 N_3H peak as a function of pH of a 3 mM solution of HRP–CN in ^1H_2O at 35 °C in the absence (○) and in the presence of a 20-fold excess of BHA (●). Note that the base-catalyzed exchange with bulk solvent in the absence of substrate is completely suppressed by BHA binding.

(not shown) which have been assigned to the distal His 42 N_3H and N_1H, respectively (Thanabal et al., 1988a). Upon addition of excess BHA, the labile proton peaks exhibit only minor shifts (Table II). A plot of the His 42 N_3H line width as a function of pH is illustrated in Figure 4. In the pH region 4–7, the line width of 110 ± 10 Hz is pH independent and consistent with solely dipolar relaxation by the iron (Thanabal et al., 1988a). At alkaline pH, the line width increases sharply with pH, indicative of the onset of a base-catalyzed exchange process in the slow-exchange limit (Lecomte & La Mar, 1985). Saturation of the solvent resonance leads to saturation transfer to the N_3H peak, establishing that the dynamic process involves exchange with bulk water (not shown). The line width increase at alkaline pH is clear evidence of exchange by the EX_2 mechanism (Woodward et al., 1982) described by eqs 2 and 3. The estimated exchange rate at pH 8.8 in the absence of BHA based on an observed line width of ~500 Hz (and a 110-Hz line width in the absence of exchange), yields $k_{obs} = 1.2 \times 10^3$ s^{-1} via eq 4. This rate is that expected for an open channel ($K_{op} \sim 1$ in eq 2), since a diffusion controlled $k_2 \sim 10^{10}$ M^{-1} s^{-1} predicts an exchange rate at pH 8.8 within a factor of 10 for that observed.

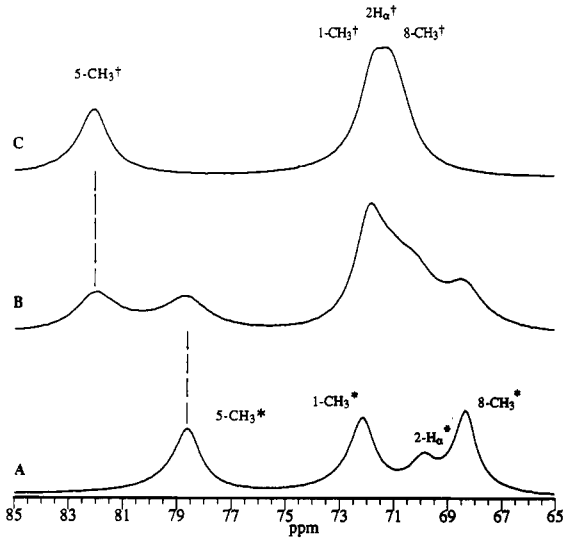

FIGURE 5: Dynamics of BHA binding to HRP: 300-MHz ^1H trace of 3 mM HRP in ^2H_2O, pH 6.8, at 35 °C (A) in the absence of BHA, (B) upon addition of ~0.5 equivalent of BHA to convert half of the resting-state complex to BHA·HRP, and (C) upon addition of an excess of BHA to completely convert the sample to BHA·HRP. The resonances of HRP and BHA·HRP are labeled by * and †, respectively. Note the excess broadening (by ~220 Hz) of the 5-CH_3* and 5-CH_3† peaks for the 1:1 BHA·HRP:HRP ratio (trace B) over that in either pure HRP (trace A) or pure BHA·HRP complex (trace C).

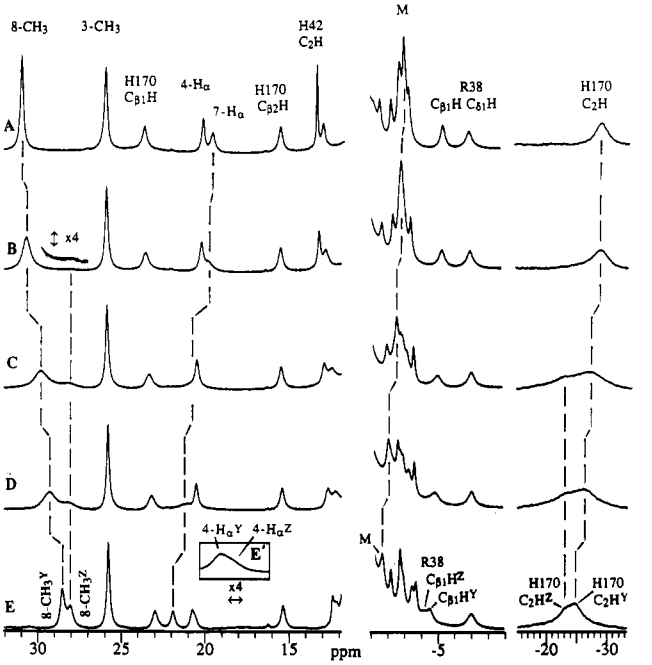

FIGURE 6: Titration of HRP–CN with BHA to form heterogeneous BHA·HRP–CN complex. Resolved portion of the 500-MHz ^1H NMR spectrum of 3 mM HRP–CN (with a 20-fold excess of CN^-) in ^2H_2O, pH 6.8, at 25 °C, (A) in the absence of BHA, and in the presence of BHA with BHA:HRP–CN ratios of (B) 0.2, (C) 0.6, (D) 0.8, and (E) 10.0. The trace in (E) is unaffected upon further addition of BHA (or CN). The vertical scale for the −15 to −35 ppm portion is expanded by a factor of 5 relative to the remainder of the spectrum. The assignments for HRP–CN are given in trace A. The dashed lines illustrate the shift changes experienced by the HRP–CN resonances upon BHA binding. Note that for two resonances, the heme 8-CH_3 and His 170 C_2H, addition of BHA causes both shift of the resonance (and intensity loss) and the appearance of a second resonance for each (8-CH_3^Z, His C_2H^Z) whose intensity increases with invariant shift as the BHA:HRP–CN ratio increases. Careful inspection shows that the 3:2 heterogeneity is also observed in the fully formed BHA·HRP–CN complex for the vinyl 4-H_α (insert E′ with factor 4 expanded horizontal scale), and Arg 38 $C_\beta H$. Moreover, the methyl peak M from Ile-X exhibits reduced intensity in trace E as compared to the 3-CH_3 peak but has intensity comparable to 8-CH_3^Y, which indicates that M also experiences the microheterogeneity.

The addition of BHA does not alter the distal His 42 N_3H line width at low pH (Figure 4). Moreover, this line width remains independent of pH to 8.8. Estimating a <10-Hz exchange contribution at pH 8.8 (Figure 4) yields a $k_{obs} < 30$ s^{-1} in the presence of BHA. Thus, the distal His labile proton exchange rate is significantly retarded (by a factor >40) by the binding of BHA by reducing K_{op} by >40. Since $\Delta G = -RT \ln K_{op}$, the >40-fold decrease in K_{op} upon BHA binding translates into a >2.2 kcal/mol destabilization of the open channel relative to the substrate-free complex (Woodward et al., 1982; Lecomte & La Mar, 1985). For all of the distal His N_3H line width measurements, care must be taken to ensure that the BHA·HRP–CN complex dominates at all pH values, as confirmed by the pH-independent 8-CH_3 peak at 29.8 ppm at 35 °C. This is important since only the protonated BHA binds to the enzyme, and the pK is ~8.8 (Schonbaum, 1973). However, a 20-fold excess of BHA guarantees saturating the substrate binding site even at pH 8.8, as evidenced by both the 8-CH_3 shift and line width characteristic of the completely formed BHA·HRP–CN complex.

Dynamics of BHA Binding to HRP. It had been reported that the titration of resting-state HRP with BHA at 21 °C leads to progressive loss of the peaks characteristic of HRP with the replacement of a set of resonances for the BHA·HRP complex (Morishima & Ogawa, 1979). Portions of the 35 °C ^1H NMR spectra of HRP upon addition of 0.0, 0.5, and 1.0 equivalent of HRP are shown in Figure 5A–C. Peaks for pure HRP and the BHA·HRP are labeled by * and † superscripts, respectively. Careful analysis reveals that each of the 5-CH_3 peaks in Figure 5B is ~220 Hz broader than either in the absence of BHA or in the presence of excess BHA. Carrying out the same titration at 55 °C reveals that the 5-CH_3* (HRP) and 5-CH_3† (BHA·HRP) peaks are in fast chemical exchange, with a maximum width when the average chemical shift is midway between that of HRP and BHA·HRP, with a line width 7×10^2 Hz greater than that of either 5-CH_3 peak in the absence of exchange (not shown). The fast exchange limit allows analysis via eq 6 which, with the 950-Hz shift difference, yields a mean exchange rate ~1.9×10^3 s^{-1} at 55 °C. The excess line broadening of ~220 Hz in the slow-exchange limit at 35 °C (Figure 5B) yields (via eq 4) a mean exchange rate ~ 6.9×10^2 s^{-1}. Extrapolation of the 55 and 35 °C rates assuming Arrhenius behavior yields a rate ~ 4×10^2 s^{-1} at 25 °C which can be attributed to the k_{off}(BHA) and is included in Table I. The published $K_4 = 2.4 \times 10^{-6}$ M at 25 °C (Schronbaum, 1973), together with the determined k_{off}(BHA) ~ 4×10^2 s^{-1}, yields k_{on}(BHA) = 1.7×10^8 M^{-1} s^{-1}; this value agrees reasonably well with an earlier estimate of 4×10^7 M^{-1} s^{-1} (Schonbaum, 1973).

Effect of CN^- on BHA Affinity. The influence of BHA binding on the low-field 220-MHz ^1H NMR spectra of HRP–CN at 21 °C had been reported to lead to an averaged spectrum reflecting BHA exchange fast on the NMR time scale (Morishima & Ogawa, 1979). The present 500-MHz ^1H NMR data in Figure 2 demonstrate that ligation of CN^- at 25 °C to the preformed BHA·HRP complex (in the presence of excess BHA) leads to two forms of the BHA·HRP–CN complex with clearly resolved 8-CH_3 peaks (see below). The 25 °C titration of BHA to the preformed HRP–CN complex (in the presence of excess CN^-) is illustrated in representative ^1H NMR traces in Figure 6. The plot of chemical shift changes for all resolved resonances as a function of BHA is presented in Figure 7. In general, all HRP–CN peaks exhibit shift

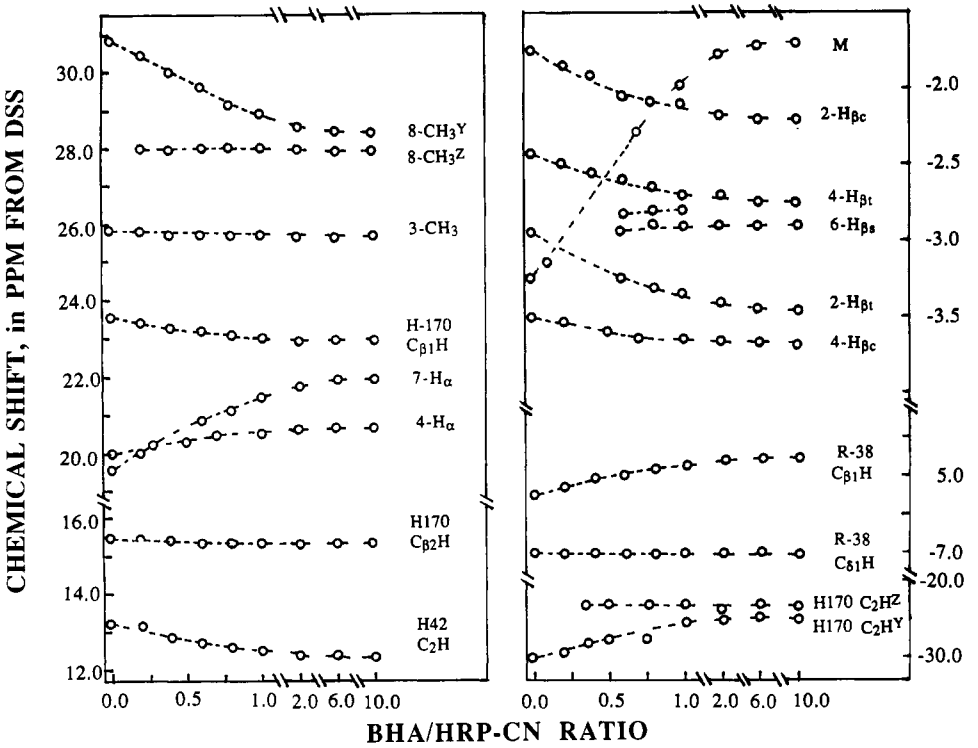

FIGURE 7: Chemical shift titration of HRP–CN with BHA. Plot of observed chemical shift, referenced to DSS, for 3 mM HRP–CN upon increasing BHA concentration as given by the BHA:HRP–CN ratio at pH 6.8 and 25 °C. This titration allows the deconvolution of the overlapping resonances in the 0 to –4 ppm region. Note that 8-CH_3 and His 170 C_2H display two resonances at this temperature, one with invariant shift and one which depends on the BHA:HRP–CN ratio. Hence, the two complexes of BHA·HRP–CN, designated Y and Z, exhibit different exchange dynamics for BHA.

change with increasing BHA, with some total shifts very small, while others approach 2 ppm (Table II). However, for the 8-CH_3 peak (as well as the less well resolved His 170 C_2H), which shows the largest shift change and also exhibits two environments in the final BHA·HRP–CN, the behavior with [BHA] is remarkable. The 8-CH_3 peak moves upfield with [BHA] and concomitantly a new 8-CH_3 peak (designated 8-CH_3^Z) grows with chemical shift 28.0 ppm essentially independent of [BHA]. The increase in this 8-CH_3^Z peak intensity is at the expense of the other 8-CH_3 peak that changes shift and broadens with [BHA]. In the presence of excess BHA (Figure 6E), a spectrum is obtained whose shifts, line widths, and relative peak areas are independent of further addition of either CN^- or BHA. We designate the two forms of the BHA·HRP–CN complex as Y and Z with the 25 °C 8-CH_3 peaks at 28.4 (8-CH_3^Y) and 28.0 ppm (8-CH_3^Z), respectively (Table II). The initial HRP–CN complex is designated A with the 8-CH_3 peak at 30.9 ppm (8-CH_3^A). The upfield His 170 C_2H peak exhibits a similar behavior. Moreover, the 4-H_α, Arg 38 $C_\beta H$, and methyl peak M, proposed to arise from $C_\delta H$ of an unassigned Ile, are also split to reflect the Y,Z heterogeneity (Figure 6 and Table II).

The titration of HRP–CN with BHA must therefore be represented by two equilibria:

$$(\text{BHA·HRP–CN})^Y \rightleftarrows (\text{HRP–CN})^A + \text{BHA} \quad (8)$$

$$(\text{BHA·HRP–CN})^Z \rightleftarrows (\text{HRP–CN})^A + \text{BHA} \quad (9)$$

The shift-invariant 8-CH_3^Z peak characterizes the Z-complex environment. The 8-CH_3 peak which shifts in position with BHA represents the averaged 8-CH_3^A/8-CH_3^Y environments. Thus, one equilibrium is slow on the NMR time scale with line width governed by eq 4, while the other is fast on the NMR time scale with line width governed by eq 5. The mole fraction complex Z is given by the intensity of the 8-CH_3^Z peak over the sum of the 8-CH_3^Z and averaged 8-CH_3^A/8-CH_3^Y intensities. The relative fractions of complex A and Y are readily determined from the peak areas and 8-CH_3 shift positions. The ratio of Y:Z is 1.7 ± 0.2 in the fully formed BHA complex on the basis of the relative areas of the 8-CH_3^Y and 8-CH_3^Z peaks in Figure 6E. Under fractional BHA binding, for example in Figure 6C, the area of 8-CH_3^Z indicates ~0.2 mole fraction of complex Z; moreover, the averaged 8-CH_3 shift for the other peak indicates comparable amounts of A and Y ~ 0.4. Therefore, the estimated ratio of Y:Z of ~2 under only fractional binding of BHA is similar to that in the fully formed BHA complex and supports the conclusion that the binding constants of BHA for complex Y and Z are very similar, i.e., $K_1^Y \sim K_1^Z \sim 1.5 \times 10^{-4}$ M, as determined earlier (Schonbaum, 1973).

Thus, BHA binding to HRP–CN is heterogeneous and must represent two modes of substrate binding. These two heterogeneous ternary complexes, however, exhibit very similar thermodynamics for cyanide (Figure 2) and BHA (Figure 6) binding. Note that it is not possible to determine if $k_{off}[CN^-]$ differs for the Y and Z complex of BHA·HRP–CN since these data can only be measured at ≥55 °C by saturation transfer and at this temperature the environments of Z and Y are completely averaged (see below).

Dynamics of Ternary Complex Heterogeneity. The ^1H NMR spectra of the complexes Y and Z of BHA·HRP–CN, under conditions where added BHA or CN^- does not influence any spectral parameters, exhibit a temperature dependence as illustrated in Figure 8. As the temperature is lowered, the ratio of 8-CH_3^Y:8-CH_3^Z intensity decreases, with an estimated 1.1 ± 0.1 ratio at 5 °C. Below 25 °C, the 8-CH_3^Y and 8-CH_3^Z peaks narrow slightly and then broaden again slightly at 5 °C, where their widths of ~190 ± 20 Hz are essentially the same as for the single 3-CH_3 peak. The narrowing of the 8-CH_3 peak on going from 25 to 15 °C, however, demands that the excess line broadening at 25 °C arise from the interconversion

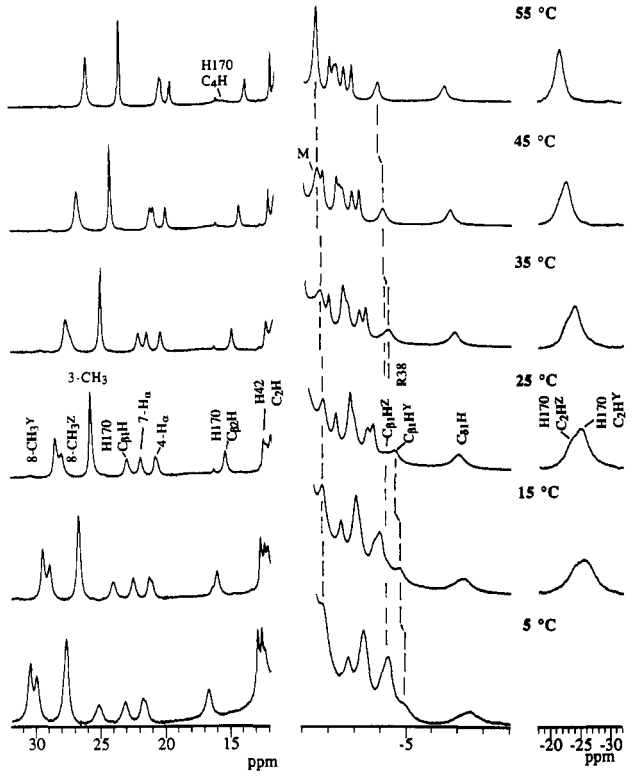

FIGURE 8: Dynamic averaging of the microheterogeneity of the ternary BHA·HRP–CN complex. Temperature dependence of the resolved portions of the 500-MHz ^1H NMR trace of fully formed 3 mM BHA·HRP–CN in ^2H_2O, pH 6.8, in the presence of a 10-fold excess of BHA and a 20-fold of excess CN^-. Raising the temperature dynamically collapses the various pairs of peaks for the Y and Z complexes (8-CH_3, 4-H_α, His 170 C_2H, Arg 38 $C_\beta H$, and Ile-X methyl peak M). Note that upon lowering the temperature from 45 to 35 °C, the 8-CH_3 and Ile-X methyl peak M become asymmetric, due to the freezing out of the microheterogeneity.

between the Y and Z complexes of BHA·HRP–CN. This is supported by the variable temperature data in Figure 8 where the 8-CH_3 peaks coalesce into a single line whose width asymptotically approaches that of the 3-CH_3 peak at high temperature. It is also noted that several other resonances exhibit the heterogeneity reflected in the Y,Z complexes, namely the heme 4-H_α, Arg 38 $C_\beta H$ and His 170 C_2H among the resolved resonances (Table II), and the upfield amino acid methyl peak, M (see below), which has been attributed to an Ile at the heme periphery near the 8-CH_3 site (de Ropp et al., 1991). At elevated temperatures, all of the split resonances coalesce and narrow to yield resonances with line widths approaching the values for the same resonance in the HRP–CN complex in the absence of BHA. Assuming that the 8-CH_3^Y:8-CH_3^Z line widths in the absence of Y $\rightleftarrows$ Z interconversion are the same as that of the 3-CH_3 at 25 °C (i.e., 100 ± 10 Hz), the 65 ± 25 Hz broadening of 8-CH_3^Y, 8-CH_3^Z peaks in the slow exchange limit at 25 °C relative to 3-CH_3 yields (eq 4) an interconversion rate of $\sim 2 \times 10^2$ s^{-1}.

Dynamics of BHA Binding to HRP-CN. Under nonsaturating BHA conditions, the 8-CH_3 peaks of both the Y and Z complexes of BHA·HRP–CN exhibit extensive line broadening at 25 °C considerably over that characterized for the direct Y $\rightleftarrows$ Z interconversion (see above) and must reflect the rate of BHA binding to the HRP–CN complex. Moreover, in spite of very similar K_1 binding constants of BHA for complexes Y and Z, the BHA off-rates differ substantially (see below). The mean lifetime for the bound BHA in each complex is most readily determined under conditions where the interconverting species are comparably populated (Sandström, 1982) (eq 6). For the A $\rightleftarrows$ Y equilibrium, this is shown in Figure 6C where the assigned 8-CH_3 peak is midway between the pure 8-CH_3^A and 8-CH_3^Y peaks. The observed line width at this BHA ratio (which is also the maximum width for the averaged signal as a function of BHA concentration) is 460 ± 50 Hz, while that of 8-CH_3^A (no BHA, Figure 6A) is only 100 ± 10 Hz and that of 8-CH_3^Y (excess BHA, Figure 6E) is 150 ± 15 Hz. With a chemical shift difference of 1.2 kHz (2.4 ppm at 500 MHz), eq 6 yields a mean lifetime of 1.5×10^{-4} s or a BHA dissociation rate, k_{off}^Y(BHA), $\sim 6.7 \times 10^3$ s^{-1}. Figure 6D has the amounts of A (HRP–CN) and complex Z (BHA·HRP–CN)^Z approximately comparable (one fourth mole fraction of complex A and Z, and half mole fraction complex Y, with averaged 8-CH_3 shift two-thirds of the way to that of 8-CH_3^Y). The partially overlapped resonances deconvolute into two resonances with a ~350 ± 50 Hz width for the 8-CH_3^Z peak. The line width of ~100 Hz in the absence of exchange, together with eq 4, yields a mean bound BHA lifetime of 1.3×10^{-3} s, or k_{off}^Z(BHA) $\sim 7.8 \times 10^2$ s^{-1}.

Since the BHA binding constants, K_1^Y and K_1^Z, were found to be comparable, the factor ~9 faster BHA off-rate for complex Y dictates that its on-rate is also a factor ~9 faster than for complex Z. *Thus, the heterogeneous BHA·HRP–CN complexes differ primarily in that the BHA binding is approximately an order of magnitude more labile for one than the other complex.* Using the published $K_1 \sim 1.5 \times 10^{-4}$ M (Schonbaum, 1973), the above k_{off} rates yield k_{on}^Y(BHA) $= 4.5 \times 10^7$ M^{-1} s^{-1} and k_{on}^Z(BHA) $= 5.2 \times 10^6$ M^{-1} s^{-1}. The equilibrium constants and rates determined herein are listed in Table I.

NOE Studies of BHA Binding. Previous 1D NOE studies at 55 °C had shown that the 8-CH_3 of BHA·HRP–CN yields a transferred NOE to BHA resonances (Thanabal et al., 1987b). Extension of the 1D saturation studies to other resolved resonances at 40 °C (Figure 9) reveals transferred NOEs not only from 8-CH_3 (Figure 9B) but from 7-H_α as well (Figure 9C), indicating that BHA makes comparable contact with the substituents on pyrrole D. The individual BHA (1) resonances were assigned via a COSY map designed to detect narrow lines and suppress the broad protein lines; the assignments are given in the middle portion of the reference trace in Figure 9A. The apparent larger intensity of the ortho-H signal is due to the shorter T_1 and likely closer proximity to the iron (Sakurada et al., 1986), with the slower relaxing meta-H and para-H partially steady-state-saturated at the relatively rapid pulse repetition rate of 2 s^{-1}. However, while saturating the 3-CH_3, 4-H_α, proximal His 170 C_βHs, and distal Arg 38 $C_\beta H$ and $C_\delta H$ resonances failed to yield detectable NOEs to BHA (not shown), saturation of the distal His C_2H peak exhibits a small but clearly transferred NOE to BHA (Figure 9D). Repeating the saturation of the resolved components of the 8-CH_3 peak for complexes Y and Z of the BHA·HRP–CN complex at 20 °C, reveals similarly sized transferred NOEs to BHA, indicating that the orientation of BHA is similar (not shown).

The non-heme resonance of HRP–CN which exhibited the largest fractional hyperfine shift change upon substrate binding, the upfield methyl peak labeled M, is not sufficiently resolved to carry out the 1D saturation experiments in order to assess whether methyl M makes dipolar contact with the substrate. Recent 2D studies of HRP–CN have proposed that M originates from the $C_\delta H_3$ of an as yet unspecified Ile X (de Ropp et al, 1991). This methyl has been shown by 1D NOEs to be close to both the heme 8-CH_3 group and the His 170 C_2H (Thanabal et al, 1987b). Further evidence for the participation of Ile X in substrate binding is obtained from

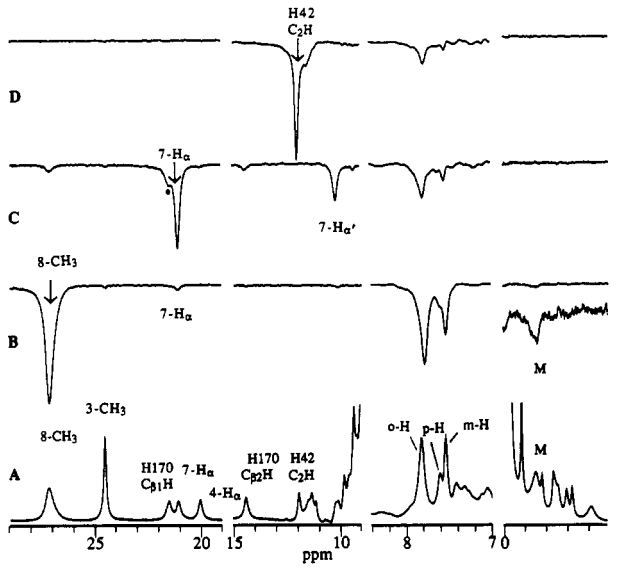

FIGURE 9: Protein–substrate contacts in BHA·HRP–CN: (A) 500-MHz ^1H NMR spectra of the fully formed 3 mM BHA·HRP–CN complex in the presence of a 10-fold excess of BHA and a 20-fold excess of cyanide in ^2H_2O, pH 6.8, at 40 °C. At this temperature, the dynamic averaging of the Y and Z complexes leads to significant 8-CH_3 line broadening. The assigned resonances of the ternary complex are labeled. The expanded horizontal scale and reduced vertical scale of the aromatic region show the BHA (**1**) resonances, as assigned by a 2D COSY experiment. Traces B–D are NOE difference traces obtained by subtracting from a spectrum with the peak of interest saturated (indicated by ↓) one with the decoupler well off-resonance; off-resonance saturated peaks are marked by ·. The averaged 8-CH_3 peak is saturated; note expected NOE to 7-H_α, as well as to a significantly broadened methyl peak M, assigned to an unknown Ile-X. The excess broadening and asymmetry of peak M is evidence that is also experiences the microheterogeneity in the BHA·HRP–CN complex. The transferred NOEs to all the protons of free BHA via BHA exchange have been reported previously (Thanabal et al., 1987b). (C) The 7-H_α is saturated, note NOE to 8-CH_3 and geminal partner 7H_α', as well as transferred NOEs to free BHA. (D) The distal His 42 C_2H is saturated; note transfered NOEs to primarily ortho-H of free BHA. Controls involving saturating slightly upfield and downfield of this peak confirm the origin of the transferred NOE as His 42 C_2H.

the variable temperature data in Figure 8, which reveal that the peak M is narrow at high temperatures (Figures 8; 45 and 55 °C) as found in pure HRP–CN, but broadens sharply at intermediate temperatures (Figure 8; 25 °C), and becomes narrow again at low temperatures (Figure 8; 15 °C) relative to the line width and shift of the invariant 3-CH_3 peak. Moreover, at the lowest temperature, the narrowed methyl peak M appears to have significantly less intensity than expected for a methyl; its intensity, in fact, is closer to that of the 8-CH_3^Y peak. At 35 °C (Figure 8), there is evidence that just after it reaches its maximum width, peak M splits into two resonances, with the weaker one (M^Z) largely lost under the upfield shoulder of the diamagnetic envelope.

Methyl peak M in HRP–CN has been shown to yield a moderate NOE upon saturating the heme 8-CH_3; it was the only NOE observed upfield of 0 ppm (Thanabal et al., 1987b). Saturation of the 8-CH_3 peak at 40 °C yields a NOE to the broadened peak M (Figure 9B). Repeating this experiment at 20 and 5 °C (not shown) where the 8-CH_3 peak is split into the 8-CH_3^Y and 8-CH_3^Z components suggests NOEs to two resonances upfield of 0.0 ppm, one each associated with one of the 8-CH_3 components; the low-field 8-CH_3^Y is connected to the more upfield M^Y, while 8-CH_3^Z is connected to the unresolved M^Z. Hence, methyl peak M experiences the microheterogeneity in the BHA·HRP–CN complexes. Moreover, the only other resonance which exhibits a substantial splitting for the complex Y:Z heterogeneity is the strongly upfield shifted proximal His C_2H peak (C_2H^Y, C_2H^Z), as clearly illustrated in the 15 and 25 °C spectra in Figure 8. The general line broadening for all resonances observed at the lower temperature, as well as the broadening from the Y/Z heterogeneity, provided insufficient sensitivity at this time to follow the substrate-bound resonances by 2D NMR in a manner reported for HRP–CN (de Ropp et al., 1991).

DISCUSSION

Interplay of Ligand and Substrate Affinity. The binding of either BHA or CN^- destabilizes the binding of the other by ~3 kcal/mol. A direct steric interaction is deemed very unlikely since the CN^- binds at the iron and BHA relaxation studies have been analyzed to place the aromatic ring of BHA > 8 Å from the iron (Sakurada et al., 1986). An indirect steric effect transmitted via a distal residue cannot be completely discounted; however, the observed *decrease* in $k_{off}(CN)$ upon BHA binding argues against it. A direct electronic origin of the interaction also seem improbable. The ^1H NMR spectral characteristics of both HRP and HRP–CN are minimally perturbed upon BHA binding.

An internally consistent rationalization for the interaction of the binding of BHA and CN^- can be obtained upon considering the close structural homology of BHA (**1**) to the most effective oxidant of HRP, aromatic peracids (**2**) (note identical disposition of potential hydrogen bonding proton relative to aromatic ring), the difference in the state of protonation of distal residues in HRP and HRP-CN, and the unique properties of BHA as a substrate of HRP. In resting-state HRP (Thanabal, 1988a) as in *Cc*P (Poulos & Kraut, 1980; Finzet et al., 1984), the distal His side chain is neutral, and hence capable of serving as a hydrogen bond acceptor toward BHA. The binding of anions, X^-, to the ferric ion in HRP is invariably accompanied by the binding of a proton; in fact, it is frequently considered that HX, rather than X^-, is the agent that binds to the iron (Dunford & Stillman, 1976). The X-ray structure of the fluoride complex of *Cc*P suggests a proton attached to the F (Edwards et al., 1984). In the case of CN^- binding, however, detailed ^1H NMR studies have established that the accompanying proton is transferred to the distal His 42 in HRP–CN to yield an imidazolium side chain that serves as a strong hydrogen bond donor to, and stabilizes the binding of, the coordinated cyanide (Thanabal et al., 1988a). Therefore, the distal His in HRP–CN, unlike HRP, is unable to serve as a hydrogen bond acceptor and would destabilize the binding of BHA. Thus, HCN and BHA would compete for the proton acceptor site on the distal His 42, and this competition accounts for their reciprocal destabilizing influence on binding constants (K_1 increased relative to K_4, K_3 increased relative to K_2).

It is noted that the binding to resting-state HRP of other substrates such as *p*-cresol and indolepropionic acid is much weaker than for BHA and that the binding constants (~2–4 mM) for the former substrates are essentially unaffected by cyanide ligation (Morishima & Ogawa, 1979). The hydrogen bonding of BHA to His 42 in BHA·HRP, but not in BHA·HRP–CN, therefore accounts both for the uniquely strong binding to HRP relative to other substrates and for the competition with cyanide binding. A pictorial representation of a binding pocket that accounts for the BHA/CN^- interaction is shown in Figure 1. The hydroxamic acid side chain is oriented such as to allow the hydrogen bond to the distal His 42 N_3H of HRP (Figure 1B). Upon cyanide bonding, His 42 becomes protonated prior to BHA binding (Thanabal et al., 1988a), and the acceptor site for BHA is abolished (Figure

1C). Aromatic substrates with other side chains stabilize the aromatic moiety in the same hydrophobic pocket near the heme edge, but the side chains do not have the appropriate length and/or geometry to make the hydrogen bond to His 42, hence their lower binding constants to HRP. It is noteworthy that aromatic peracids (**2**) have essentially identical geometry with respect to the hydrogen bonding proton relative to the aromatic ring. Thus the initial binding of aromatic peracids should resemble that of BHA, with the aromatic group near the heme edge, and the COOH hydrogen bonded to the distal His 42. Since the proposed catalytic role of the distal His is to serve as a proton acceptor for the peroxide (Poulos & Kraut, 1980), the proposed binding mode of BHA provides a ready rationalization for why an aromatic peracid is the optimal oxidant of HRP; the leaving proton is properly placed for transfer.

Influence of Cyanide Binding on BHA Dynamics. The comparison of the dynamics of BHA binding to HRP with that in HRP–CN is complicated by the presence of two BHA·HRP–CN complexes which exhibit similar binding constants for either CN^- or BHA but exhibit very different BHA exchange rates. It could not be established if their CN^- off-rates differ. For the dynamically more stable complex Z, the increase in K_1 relative to K_4 originates primarily from a decrease in k_{on}(BHA) for the ternary complex, with the k_{off}(BHA) essentially unchanged (Table I). The dynamically less stable BHA·HRP–CN complex Y also exhibits a significantly faster (factor $\sim$10) k_{off}(BHA) relative to BHA·HRP. The increased k_{off}(BHA) in the Y complex of BHA·HRP–CN relative to that in the BHA·HRP complex is consistent with the loss of the hydrogen bond (to His 42) stabilization in the former complex. The unchanged K_1 for Y relative to Z is due to the fact k_{on}(BHA) is also decreased by $\sim$10 relative to that for BHA·HRP. A plausible interpretation of this decrease in both rates in complex Z relative to those in complex Y (Table I) is considered below.

Influence of BHA Binding on Cyanide Dynamics. The influence of BHA binding on the cyanide ligation dynamics is much more complicated than that predicted simply by the hydrogen bond to His 42. Thus, BHA lowers the CN^- on-rate by $>2 \times 10^3$ (Table I). A portion, but not all, of this reduction can be attributed to a proposed structural change in the resting-state HRP induced by BHA binding. Resonance Raman studies have lead to the proposal that BHA binding to HRP converts the five-coordinate HRP to a six-coordinated BHA·HRP with a coordinated water molecule (Smulevich et al., 1991). The coordination of water to the iron in high-spin ferric myoglobins has been shown to lead to a 10^2–10^3 decrease in the anion binding on-rates (Giacometti et al., 1981). In the present case, however, the reduction in k_{on}(CN) due to BHA is greater than this $\sim 10^2$ by another factor >10. Moreover, the k_{off}(CN) is also smaller by a factor >10 upon BHA binding. This factor >10 decrease in k_{off}(CN) upon BHA binding, with a concomitant decrease in k_{on}(CN), suggests that the cyanide dynamics are modulated not only by the competitive hydrogen bonding to His 42 but also by some "gating" phenomenon that slows both rates by $\sim$10. Hence the binding site of BHA appears to "block" or close the ligation channel to the iron, or the BHA acts as a "gate" to the entering and exiting cyanide ion. Interestingly, the binding of NO_3^- at the non-iron anion binding site at pH 4 similarly retards the CN^- ligation dynamics without significantly influencing K_2 (Araiso & Dunford, 1981).

Additional support for such a modulation of the ligation channel opening can be drawn from the exchange rate with water of the distal His 42 N_3H. Such an exchange is base catalyzed and must allow OH^- access to the pocket (Woodward et al., 1982; Lecomte & La Mar, 1985). Addition of BHA reduces the exchange rate by a factor >40 (Figure 4), indicating that the probability for an open channel to the iron is significantly reduced by BHA binding. This result is reasonable since the His 42 N_3H is hydrogen-bonded to the bound cyanide (Thanabal et al., 1988a). The present NMR data are qualitatively consistent with the observation on CO geminate recombination of reduced HRP–CO. The binding of BHA was shown to increase the fraction of geminate recombination upon flashing off the CO, and this was interpreted as resulting from the prevention of CO escape from the pocket by BHA (Berinstain et al., 1990).

The Substrate Binding Site. The detailed 1D and 2D studies of HRP–CN have shown (Thanabal et al., 1987a,b, 1988a; de Ropp et al, 1991) that the orientation of the proximal His 170, as well as distal His 42 and Arg 38 relative to the heme, are essentially the same as in *Cc*P (Poulos & Kraut, 1980; Finzel et al., 1984), as shown in Figure 1. The 1D NOE data presented in Figure 9 generally support the BHA binding picture in Figure 1. The observation of transferred NOEs from the 7-H_α as well as the 8-CH_3 group to the bound BHA localizes the binding pocket closer to pyrrole D than pyrrole A. The phenylhydrazine suicide inhibitor attacks exclusively the δ-meso position (Ator & Oritz de Montellano, 1987; Ator et al., 1987). However, the isolation of some 8-hydroxymethylene (Ator & Ortiz de Montellano, 1987), but not 1-hydroxymethylene, derivatives of protohemin confirms the greater importance of pyrrole D contacts to substrate. The observation of transferred NOEs from the assigned distal His 42 C_2H to the BHA is clear evidence that the substrate binding site extends to the distal pocket. A similar conclusion has been reached by Veitch and Williams (1991). The absence of transferred NOEs from the distal Arg 38 is consistent with the position of the His 42 C_2H relative to the pyrrole D found in the *Cc*P crystal structure (Poulos & Kraut, 1980). The larger transferred NOEs to the meta-H and para-H relative to the ortho-H signals of BHA upon saturating pyrrole D substituents, compared to when His 42 C_2H is saturated, is consistent with the orientation of BHA with the aromatic ring near pyrrole D and the polar side chain near the distal His 42, as shown in Figure 1C. However, any detailed interpretation of transferred NOEs will first require elucidation of the nature of the microheterogeneity of the BHA binding site and the elucidation of the relaxation properties of each proton.

Thus, the substrate binding pocket in HRP does not appear to be sterically blocked from the ferryl oxo group, and the substrate disposition relative to the iron center does not appear to preclude oxo atom transfer to the substrate. This conclusion is consistent with the observation of incorporation of the ferryl oxo atom into sulfur-containing substrates (Doerge et al., 1991). Thus, the stereochemical disposition of the substrate binding site relative to the iron may not be the most crucial factor for differentiation between peroxidase and monooxygenase activity (Ortiz de Montellano, 1987).

The Microheterogeneity in BHA·HRP–CN. While the quantitative description of both the binding pocket and its heterogeneity is not yet attainable, the present data do provide some suggestions as to what may be happening. Since the transferred NOEs from the split 8-CH_3^Y, 8-CH_3^Z peaks to the BHA are essentially the same, the microheterogeneity must reflect alternate orientations of a binding pocket residue(s), rather than of the substrate itself within a fixed binding pocket. This is indicated by the fact that the methyl peak M, assigned to an Ile-X near the 8-CH_3 group (de Ropp et al., 1991), exhibits a very large fractional paramagnetic

shift difference between the complexes Y and Z of BHA·HRP–CN (Table I). Moreover, the only other resolved resonance which exhibits a significant shift difference between the Y and Z complexes is the proximal His 170 C_2H. Previous 1D NOE studies have revealed that the methyl M is close to both the heme 8-CH_3 and the His 170 C_2H (Thanabal et al., 1987b). Thus, M must arise from an Ile-X residue near the heme edge, but with the δ-methyl near the proximal side. However, since the NOE between this 8-CH_3 and M is seen in both the Y and Z components of BHA·HRP–CN, it is unlikely that it is Ile-X which adopts the alternate orientation. The nature of the two orientations and the identity of the residue are still to be determined. However, we propose that the residue responsible for the microheterogeneity does not sterically interact with the substrate but that its two orientations differ in that one (the minor or Z component) partially blocks the substrate binding channel. Such a microheterogeneity would account for unchanged BHA binding constants to HRP–CN for the Z and Y complexes, but k_{on}(BHA), k_{off}(BHA) rates a factor ~10 slower for the Z than the Y complex of BHA·HRP-CN.

A possible candidate for the residue with alternate orientations is one of the aromatic side chains of the proposed pair Phe 142/143 shown to interact with indolepropionic acid; the definite assignment of these resonances in the presence of BHA, however, has not been possible to date with 2D NMR studies at 30 °C (Veitch & Williams, 1991). In order to freeze out the alternate orientations for complex Y and Z, moreover, it will be necessary to extend the 2D NMR studies to even lower temperatures where the additional line broadening will seriously complicate detection of cross-peaks. However, such studies should be accessible at higher field strength (i.e., 600 MHz) and should provide considerably more insight into the details of the substrate binding properties of HRP and the nature of the presently identified heterogeneity.

ACKNOWLEDGMENT

We thank N. C. Veitch for useful discussions.

REFERENCES

Aibara, S., Kobayashi, T., & Morita, Y. (1981) *J. Biochem. 90*, 489–496.
Aibara, S., Yamashita, H., Mori, E., Kato, M., & Morita, Y. (1982) *J. Biochem. 92*, 531–539.
Araiso, T., & Dunford, H. B. (1981) *J. Biol. Chem. 256*, 10099–10104.
Ator, M. A., & Ortiz de Montellano, P. R. (1987) *J. Biol. Chem. 262*, 1542–1551.
Ator, M. A., David, S. K., & Ortiz de Montellano, P. R. (1987) *J. Biol. Chem. 262*, 14954–14960.
Atwood, J. D. (1985) Inorganic and Organometallic Reaction Mechanisms, Brooks Cole Publishing Co., Belmont, CA.
Berinstain, A. B., English, A. M., Hill, B. C., & Sharma, D. (1990) *J. Am. Chem. Soc. 112*, 9649–9651.
Burns, P. S., Williams, R. J. P., & Wright, P. E. (1975) *J. Chem. Soc., Chem. Commun.*, 795–796.
de Ropp, J. S., La Mar, G. N. (1991) *J. Am. Chem. Soc. 113*, 4348–4350.
de Ropp, J. S., Yu, L. P., & La Mar, G. N. (1991) *J. Biomol. NMR 1*, 175–190.
de Ropp, J. S., La Mar, G. N., Smith, K. M., & Langry, K. C. (1984) *J. Am. Chem. Soc. 106*, 4438–4444.
Doerge, D. R., Cooray, N. M., & Brewster, M. E. (1991) *Biochemistry 30*, 8960–8964.
Dunford, H. B. (1991) *Peroxidases in Chemistry and Biology* (Everse, J., Everse, K. E., & Grisham, M. B., Eds.) Vol. 2, pp 1–23, CRC Press, Boca Raton, FL.
Dunford, H. B., & Stillman, J. S. (1976) *Coord. Chem. Rev. 19*, 187–251.
Edwards, S. L., Poulos, T. L., & Kraut, J. (1984) *J. Biol. Chem. 259*, 12984–12988.
Ellis, W. D., & Dunford, H. B. (1968) *Biochemistry 7*, 2054–2062.
Finzel, B. C., Poulos, T. L., & Kraut, J. (1984) *J. Biol. Chem. 259*, 13027–13036.
Giacommeti, G. M., Ascenzi, P., Brunori, M., Rigatti, G., Giacometti, G., & Bolognesi, M. (1981) *J. Mol. Biol. 151*, 315–319.
Granot, J. (1982) *J. Magn. Reson. 49*, 257–270.
Gueron, M. (1975) *J. Magn. Reson. 19*, 58–66.
La Mar, G. N., de Ropp, J. S., Smith, K. M., & Langry, K. C. (1980) *J. Biol. Chem. 255*, 6646–6652.
Lecomte, J. T. J., & La Mar, G. N. (1985) *Biochemistry 24*, 7388–7395.
Leigh, J. S., Maltempo, M. M., Ohlsson, P. I., & Paul, K. G. (1975) *FEBS Lett. 51*, 304–308.
Modi, S., Behere, D. V., & Mitra, S. (1989) *J. Biol. Chem. 264*, 19677–19684.
Morishima, I., & Ogawa, S. (1979) *J. Biol. Chem. 254*, 2814–2820.
Morita, Y., Mikami, B., Yamashita, H., Lee, J. Y., Aibara, S., Sato, M., Katsube, Y., & Tanaka, N. (1991) *Biochemical, Molecular and Physiological Aspects of Plant Peroxidases* (Lobarzewski, J., Greppin, H., Penel, C., & Gaspar, T. Eds.) pp 81–88, University of Geneva Press, Geneva, Switzerland.
Ortiz de Montellano, P. R. (1987) *Acc. Chem. Res. 20*, 289–294.
Paul, K.-G., & Ohlsson, P.-I. (1978) *Acta Chem. Scand. B 32*, 395–404.
Poulos, T. L., & Kraut, J. (1980) *J. Biol. Chem. 255*, 8199–8205.
Sakurada, J., Takahashi, S., & Hosoya, T. (1986) *J. Biol. Chem. 261*, 9657–9662.
Sakurada, J., Takahashi, S., & Hosoya, T. (1987) *J. Biol. Chem. 262*, 4007–4010.
Sandström, J. (1982) *Dynamic NMR Spectroscopy*, Academic Press, London.
Schejter, A., Lanir, A., & Epstein, N. (1976) *Arch. Biochem. Biophys. 174*, 36–44.
Schonbaum, G. R. (1973) *J. Biol. Chem. 248*, 502–511.
Schonbaum, G. R. & Lo, S. (1972) *J. Biol. Chem. 247*, 3353–3360.
Smulevich, G., English, A. M., Mantini, A. R., & Marzocchi, M. P. (1991) *Biochemistry 30*, 772–779.
Thanabal, V., de Ropp, J. S., & La Mar, G. N. (1987a) *J. Am. Chem. Soc. 109*, 265–272.
Thanabal, V., de Ropp, J. S., & La Mar, G. N. (1987b) *J. Am. Chem. Soc. 109*, 7516–7525.
Thanabal, V., de Ropp, J. S., & La Mar, G. N. (1988a) *J. Am. Chem. Soc. 110*, 3027–3035.
Thanabal, V., La Mar, G. N., & de Ropp, J. S. (1988b) *Biochemistry 27*, 5400–5407.
Veitch, N. C., & Williams, R. J. P. (1991) *Biochemical, Molecular and Physiological Aspects of Plant Peroxidases* (Lobarzewski, J., Greppin, H., Penel, C., & Gaspar, T., Eds.) pp 99–109, University of Geneva Press, Geneva, Switzerland.
Welinder, K. G. (1985) *Eur. J. Biochem. 151*, 497–504.
Welinder, K. G. (1992) *Plant Peroxidases 1980–1990: Progress and Prospects in Biochemistry and Physiology* (Gaspar, T., Penel, C., & Greppin, H., Eds.) (in press).
Welinder, K. G., & Norskov-Lauritsen, L. (1986) *Molecular and Physiological Aspects of Plant Peroxidases* (Greppin, H., Penel, C., & Gaspar, T., Eds.) pp 61–70, University of Geneva Press, Geneva, Switzerland.
Woodward, C., Simon, I., & Tuchsen, E. (1982) *Mol. Cell. Biochem. 48*, 135–160.